Journal Pre-proof

Cryopreservation of implantable human skeletal muscle-derived cell-microcarrier combinations for use in clinical regenerative medicine

Chara Simitzi , Juzheng Zhang , Rainer Marksteiner , Barry Fuller , Richard Day

PII: S1465-3249(25)00842-4
DOI: https://doi.org/10.1016/j.jcyt.2025.09.005
Reference: JCYT 1982

To appear in: *Cytotherapy*

Received date: 29 July 2025
Accepted date: 10 September 2025

Please cite this article as: Chara Simitzi , Juzheng Zhang , Rainer Marksteiner , Barry Fuller , Richard Day , Cryopreservation of implantable human skeletal muscle-derived cell-microcarrier combinations for use in clinical regenerative medicine, *Cytotherapy* (2025), doi: https://doi.org/10.1016/j.jcyt.2025.09.005

Highlights

- Cryopreservation of implantable microcarriers with adherent cells is demonstrated
- Most skeletal muscle derived cells remain viable and attached to microcarriers
- Cells retain phenotypic properties after freezing and thawing
- Microcarrier physical and mechanical properties remained unchanged
- Findings support cold-chain supply for implantable cell-microcarrier products

Cryopreservation of implantable human skeletal muscle-derived cell-microcarrier combinations for use in clinical regenerative medicine

Chara Simitzi[1], Juzheng Zhang[1], Rainer Marksteiner[2], Barry Fuller[3], Richard Day[1*]

Corresponding author: r.m.day@ucl.ac.uk

Affiliations:

[1]Division of Medicine, University College London, London, United Kingdom,

[2]Innovacell GmbH, Mitterweg 24, A-6020, Innsbruck, Austria

[3]Division of Surgery, University College London, London, United Kingdom,

Abstract

Regenerative medicine therapies include tissue engineered constructs to restore tissue and organ function. Among the different approaches, implantable polymeric microcarriers have been proposed for delivery of anchorage-dependent cells to target tissue locations. Cell-microcarrier combinations produced as fresh advanced therapy medicinal products (ATMP) face significant challenges in terms of manufacturing and in time distribution. In the current study, we have explored the feasibility cryopreservation for human skeletal muscle-derived cell (SMDC) – implantable microcarrier combinations. Existing and novel cryoprotectant formulations combined with slow cooling were investigated, along with rapid and slow thawing regimens. Under specific conditions following cryopreservation and thawing, most SMDC cells were viable and remained attached to the microcarriers. Furthermore, the capacity of human SMDC to differentiate into myotubes was unaffected. The cryopreservation process did not alter the physico-mechanical properties of the microcarriers enabling them to retain their primary function of an implantable cell substrate. Overall, these findings pave the way to use cold-chain product supply for future clinical studies with the implantable cell-microcarrier technology.

Keywords:

Cryopreservation, cell microcarriers, TIPS, slow cooling, ATMP

Abbreviations[1]

[1] ATMP: Advanced Therapy Medicinal Product; CPA: Cryoprotective Agent or cryoprotectant; CS10: CryoStor10®; CS10Gr: CS10 containing GranuGel®; DMSO: Dimethyl sulfoxide; MHC: Myosin Heavy

1. Introduction

Regenerative medicine involving tissue engineered products is being developed to restore tissue and organ function for a range of conditions throughout life. A critical requirement for these therapies is to ensure that the constituent cells in the product remain viable and functional following manufacture, transportation and clinical delivery. This can be particularly challenging when using cells anchorage-dependent cells that are normally found adhered to other cells and tissues in the body. To overcome this, biomaterials-based constructs can be loaded with therapeutic cells and injected or implanted at the target location. Examples include implantable scaffolds [1], injectable hydrogels [2,3] and polymeric microcarriers [4,5].

Polymeric microcarriers are usually microspheres, with diameters ranging from 50 to 400 microns, made of biocompatible polymeric materials [such as polystyrene, poly(lactic-co-glycolic acid) (PLGA) and gelatin], that allow cell adhesion over a large surface area. Different characteristics (e.g. porosity, diameter, surface chemistry, etc.) enable cell-laden or cellularized microcarriers to have a variety of applications in regenerative medicine [6,7]. They are also used as culture substrates for cell expansion in bioreactor-based advanced 3D cell culture models [8–10], cellularized building blocks for bottom-up tissue engineering (TE) scaffolds [11–13], and as cell carriers in cell therapy applications [14,15].

Cells require detachment from conventional non-implantable microcarriers before *in vivo* transplantation [16–18]. We have previously shown the attachment and growth of anchorage-dependent cells using implantable microcarriers produced using thermally induced phase separation (TIPS). These microcarriers have been demonstrated to be compatible with *in vivo* implantation while maintaining functional properties of conventional microcarriers for the growth and differentiation of a variety of adherent cell types (skeletal muscle, mesenchymal stromal cells, induced pluripotent stem cells) [13,19–21]. The microcarriers used alone as a medical device have previously been shown to be biocompatible *in vivo* and safe when clinically implanted in humans as part of a Phase I safety study investigating their use for fistula repair (NCT03707769). More recently, the implantable microcarriers with cells attached have undergone non-clinical degradation and toxicology safety testing as part of their development towards clinical investigation as a combined ATMP for treatment of incontinence. For this approach, autologous human skeletal muscle-derived cells (SMDC) are attached to the surface of the implantable microcarriers [21]. The cell-microcarrier combination is mixed in syringes with an inert hydrogel (GranuGel®) that acts as a viscosity modifier before being distributed to clinical sites for use as a fresh product. Fresh ATMPs containing perishable cells often have a short shelf-life, typically ranging from 12 - 96 hours cells, which significantly impacts the logistics of manufacturing and distribution to clinical

Chain; PLGA: poly(lactic-co-glycolic acid); SMDC: Skeletal Muscle-Derived Cell; TIPS: Thermally Induced Phase Separation

sites. To address this challenge, storage and distribution of the combined ATMP as a cryopreserved product to the clinical site could be an option.

Cryopreservation of biological materials, such as cells or tissue fragments, is a common process used for long-term storage and transport by cooling them to cryogenic temperatures (-80 to -196 ºC) [22]. The potential to preserve and store biological materials for research or clinical use at a later timepoint makes cryopreservation an increasingly important tool in haematopoietic stem cell transplantation, cell therapy, and regenerative medicine [23–25]. Cryopreservation has been used in clinical trials in cellular immunotherapies, where therapeutically active non-adherent cells, such as T cells, are cryopreserved in the form of a cell suspension [26]. The cryopreservation process typically involves several steps including: (i) incubation with the cryoprotectant (CPA), (ii) controlled freezing, (iii) storage at cryogenic temperatures for days to years, (iv) controlled thawing/warming, and (v) removal of the CPA from the mixture. Each step has risks associated with cell damage caused by ice formation [27,28]. Accordingly, various CPA (in terms of nature, mechanism and concentration) and cooling/warming methods exist, reflecting the different parameters that affect the biophysical phenomena [22,26]. Cryopreservation of cellularized scaffold-based constructs is generally more complex than for cell suspensions because there is a need for retaining key attributes of both the attached cells and integrity of the scaffold material [29].

The current study describes the development of a cryopreservation process for the SMDC-implantable microcarrier combination. Microcarriers made of PLGA were fabricated using thermally induced phase separation (TIPS). Human SMDC from five healthy donors were attached to the surface of TIPS PLGA microcarriers using previously established methods [21] and cryopreserved using slow cooling. In addition to the standard CPA mixture (CryoStor10®; BioLife Solutions, USA; a clinically-approved DMSO-based solution), we also investigated addition of a sterile polymeric hydrogel (GranuGel®) along with different thawing conditions. Data from the study demonstrate that cryopreservation of the SMDC-implantable microcarrier combination is technically feasible under defined controlled freezing/thawing conditions. This approach may help resolve issues associated with distribution of fresh tissue engineered ATMPs removing the need for just in time supply constraints associated with fresh products.

2. Materials and Methods

2. 1. **Fabrication of TIPS PLGA Microcarriers**

Polymeric microcarriers were prepared using thermally induced phase separation (TIPS), as previously described [19]. Briefly, a 2% weight:volume (w/v) solution of poly(DL-lactide-co-glycolide) (PLGA; Purasorb® PDLG7507 75:25) in dimethyl carbonate (DMC; Sigma Aldrich) was prepared. Polymer droplets were produced using a Nisco Encapsulator Unit Var D (Nisco Engineering, Switzerland), fitted with a stainless steel, sapphire-tipped nozzle (100 µm orifice) at a flow rate of 2 ml/min and vibration frequency of 2.70 kHz (amplitude 100%). The polymer droplets were collected into liquid nitrogen to achieve thermally induced phase separation of the polymer and solvent before being lyophilized in a freeze drier (Edwards MicroModulyo) for 24 hr to achieve sublimation of the frozen solvent. After lyophilization, the dry microcarriers were sieved (Endecotts™ Stainless Steel Test Sieve, Fisher Scientific, United Kingdom) to a size range of 250-500 µm.

2.2. **Characterization of TIPS PLGA microcarriers**

The surface morphology of the microcarriers was assessed using scanning electron microscopy (SEM). Samples of TIPS PLGA microcarriers were mounted on aluminium stubs using adhesive carbon tabs and sputter coated with gold (Polaron E5000). Samples were imaged using a Hitachi S3400N scanning electron microscope at 5 keV.

To quantitatively evaluate the morphological characteristics (size and shape) of the microcarriers, a particle image analyzer (Morphologi G3; Malvern Panalytical, UK) was used. Approximately 200 microcarriers were evaluated for each parameter assessed.

2.3 Pre-conditioning of TIPS PLGA microcarriers

To promote cell attachment, microcarriers were pre-conditioned as previously described [21]. The pre-conditioning solution consisted of 10% (v/v) ethanol in proliferation medium [Ham's F-10 Nutrient Mix, GlutaMAX™ Supplement (ThermoFisher Scientific), 10% v/v fetal bovine serum (FBS; Life Sciences, USA), 1% antibiotic and antimycotic (0.25 mg/ml Amphotericin B, 100 units/ml penicillin and 100 mg/ml streptomycin) (Gibco) and 10 ng/ml human fibroblast growth factor (FGF)-basic (PeproTech, UK)]. 20 mg TIPS PLGA microcarriers were added to 7 ml polystyrene containers and incubated in 5 ml of the wetting solution under rotation at 37 ºC for 3 days. Successful pre-conditioning of the microcarriers was confirmed by their sedimentation in the container. The

microcarriers were washed twice with fresh proliferation medium and stored at 4 ºC before use in the *in vitro* experiments with cells.

2.4 Human skeletal muscle-derived cells

Human skeletal muscle-derived cells (SMDC) from five different healthy human donors were supplied by Innovacell GmbH (Austria). SMDC were isolated (following a previously established methodology, described elsewhere [30]) from muscle tissue biopsy samples from healthy donors, upon signed informed consent and following the principles of the Declaration of Helsinki and of the International Conference on Harmonization—Good Clinical Practice. Before experiments, SMDC were thawed and plated on tissue culture flasks (Sarstedt, Germany) at a cell density of 10,000 cells/cm^2. SMDC were cultured in proliferation medium (described in Section 2.3). The culture medium was changed every 2–3 days. For subculture and harvesting, cells were rinsed with Dulbecco's phosphate buffered saline (PBS; Merck), detached using trypsin-ethylenediaminetetraacetic acid (EDTA) solution (Sigma Aldrich), washed in proliferation medium and centrifugated at 190 x *g* for 5 min. The cell pellet was resuspended in fresh proliferation medium before being transferred into new tissue culture flasks for subculture or used for the experiments with the microcarriers.

2.5. In vitro attachment of cells on TIPS PLGA microcarriers

PBS-0.1 mini vertical-wheel bioreactors (PBS Biotech, Inc., USA) were used for the attachment of the cells to the TIPS microcarriers, as previously described [21]. 100 mg of pre-conditioned microcarriers and 20x10^6 SMDC (passage 5 – 9) in 60 ml proliferation medium were added into the bioreactor. The bioreactor was placed in an incubator at 37ºC and 5% CO_2 with a humidified atmosphere for 18 h. The rotation speed of the bioreactor was set at 40 rpm with an intermittent profile of 20 sec agitation per hour. At the end of the incubation period cells had attached on the microcarriers (termed as 'cellularized microcarriers').

At the end of the incubation period, the contents of the bioreactor containing the cellularized microcarriers were transferred into a 50 ml polypropylene container (Falcon®) and the cellularized microcarriers were allowed to sediment. The number of cells attached to the surface of microcarriers was indirectly quantified by subtracting the number of the non-attached cells in the supernatant [measured using an automated cell counter (NucleoCounter® NC-200, Chemometec, Denmark)] from the seeding cell number.

2.6. Incubation of the cellularized TIPS PLGA microcarriers with cryoprotectants and cryopreservation

The following cryoprotectants were investigated: i) CryoStor10® (CS10; BioLife Solutions, USA), a clinically approved commercial cryoprotectant containing 10% dimethyl sulfoxide (DMSO) or ii) CS10 mixed 1:1 with 10% (v/v) GranuGel® (ConvaTec, United Kingdom) in proliferation medium (CS10Gr; final concentration of DMS0 5% and GranuGel® 5%).

For cryopreservation, the cellularized microcarriers were washed in PBS before being resuspended in 36 ml proliferation medium, and aliquoted into three 50 ml polypropylene containers as follows: 4 ml for the control samples that were not incubated in cryoprotectant and were not cryopreserved ('before cryopreservation'), 16 ml for the CS10 samples and 16 ml for the CS10Gr samples that were further cryopreserved.

For the samples incubated in the CS10, microcarriers were left to sediment, the proliferation medium was removed, and the microcarriers were resuspended in 8 ml CS10. The cellularized microcarriers were mixed and quickly aliquoted in eight 2ml cryogenic vials (Nunc; Denmark) (1 ml of cellularized microcarriers per cryogenic vial).

For the samples incubated in the CS10Gr, microcarriers were left to sediment, the proliferation medium was removed, and the microcarriers were resuspended in 4 ml CS10. Using two Luer-lock syringes (Fisher Scientific) with a syringe connector, the cellularized microcarriers were mixed with 4 ml 10% GranuGel® (v/v) solution in proliferation medium. The 8 ml total suspension of cellularized microcarriers was quickly aliquoted into eight 2ml cryogenic vials (1 ml of cellularized microcarriers per cryogenic vial).

For the process of slow cooling, a VIA Freeze^{TM} controlled rate freezer (Cytiva, UK) with a cooling rate of -1 ^{o}C/min (after 10 min equilibration at 4 ^{o}C) was used. When the temperature reached -70 ^{o}C, the cryogenic vials were transferred to the -70 ^{o}C freezer, and next day they were transferred to the liquid nitrogen inside a box with dry ice.

A schematic diagram of the process is shown at the **Figure 1A**.

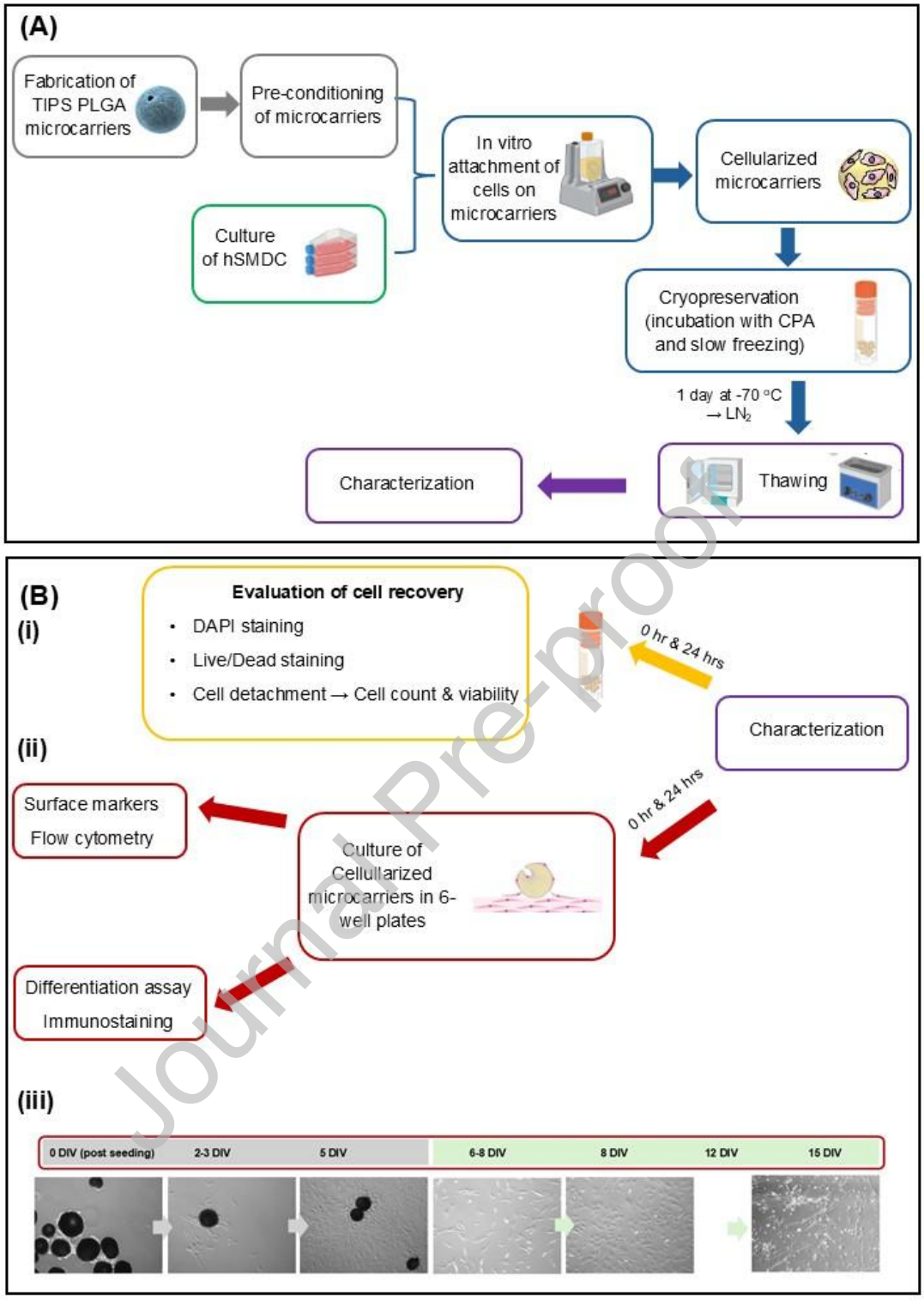

Figure 1: Schematic diagram of the experimental protocol. (A) Preparation of the cellularized implantable microcarriers. (B) Characterization of cell recovery, in terms of viability and number (Bi), surface marker expression and differentiation of the SMDC after their growth on the microcarriers (Bii); timeline of the differentiation study (Biii).

2.7. Characterization of the cellularized TIPS PLGA microcarriers after thawing

Cryogenic vials containing cellularized TIPS PLGA microcarriers were taken from storage in liquid nitrogen and transferred to the lab in dry ice for storage in a -80 ºC freezer while vials were thawed two at a time. Frozen vials were thawed at 37 ºC using two different regimes: (i) placing in water bath (rapid), or (ii) incubator (slow). Thawing in water was performed by swirling the vial in the water bath for 2 – 3 minutes. For the slow thawing, vials were placed on the shelf of the incubator for 9 – 12 minutes. In both cases, vials were transferred to the biosafety cabinet just before being completely thawed.

The contents of each vial were transferred using a Pasteur pipette into a 30 ml polystyrene container. 10 ml proliferation medium was added dropwise to the cellularized microcarriers followed by gentle mixing by inverting the container five times up and down. The cellularized microcarriers were allowed to sediment before removing the medium freezing and washing again with 5 ml proliferation medium. The cellularized microcarriers were either directly characterized ('0 hr' samples) or transferred to a low-attachment 6-well plate (Corning, UK) for 24 hr assessment ('24 hr'). Supplementary **Table 1** shows the details of the samples used in the study for characterization of cell viability and total number of cells attached on the microcarriers per cryogenic vial, cell number per microcarrier, myogenic differentiation potential and surface marker expression of the cells after migration off the microcarriers (**Figure 1B**). Details of the protocols are discussed in the following sections.

Cells from the cryopreserved cellularized microcarriers derived from all five different donors were characterized in an identical manner.

2.7.1 Quantitative evaluation of cell number and viability

To assess cell viability and total number of cells attached to the microcarriers in each cryogenic vial, the cellularized microcarriers were washed twice with PBS, and incubated for 5 min with 1.5 ml of trypsin-EDTA. To promote detachment of cells from the microcarriers, samples were gently mixed by pipetting up and down ten times. The microcarriers were allowed to sediment, and a sample of the supernatant (containing the detached cells) was measured using an automated cell counter (NucleoCounter® NC-200).

2.7.2 Quantitative evaluation of cell attachment using DAPI staining

DAPI staining was used to quantify the number of attached cells per microcarrier. A sample of the cellularized microcarriers was washed with PBS, fixed with 4% formaldehyde permeabilized with 0.1% (v/v) Triton X-100, and incubated with DAPI staining solution (NuncBlue Fixed cell staining; ThermoFisher). Cellularized microcarriers were washed twice with PBS and imaged with a fluorescence microscope (Zeiss AXIO, Germany).

2.7.3 Qualitative evaluation of viability using Live/Dead staining

For the Live/Dead staining, a sample of the cellularized microcarriers was incubated with the staining solution (LIVE/DEAD™ Viability/Cytotoxicity Kit, Invitrogen) for 30 min at room temperature. The cellularized microcarriers were washed with PBS and imaged with a fluorescence microscope (Zeiss AXIO, Germany) within the next hour.

2.7.4 SMDC differentiation and surface marker expression

A sample of the cellularized microcarriers was transferred to a standard 6-well tissue culture treated plate (Sarstedt, Germany) and incubated in proliferation medium to allow migration of the cells off the microcarriers and attachment to the bottom of the plate (Figures 1Bii and 1Biii). After 2 – 3 days, proliferation medium was replaced with fresh medium. When cells reached 80 - 90% cell confluence, the cells and microcarriers were detached with trypsin-EDTA, sieved with 100 µm Corning® cell strainers (Merck, Germany) to remove the microcarriers, and the cells were re-plated in standard in 24-well and 6-well tissue culture treated plates for immunostaining and flow cytometry, respectively.

2.7.4.1 SMDC differentiation

Cells were incubated in proliferation medium until reaching 70 – 80% confluence, after which the medium was switched to differentiation medium consisting of Dulbecco's Modified Eagle Medium F12 (DMEM F12; ThermoFisher Scientific), 1% insulin-transferrin-selenium solution (ThermoFisher Scientific), 1% N_2 supplement (ThermoFisher Scientific), 2 mM L-Glutamine (Merck) and 100 units penicillin and 0.1 mg streptomycin/ ml (Merck). After 7 days incubation in differentiation medium cells were stained for myosin heavy chain (MHC). Cells were fixed with 4% formaldehyde for 10 min, permeabilised with 0.1% (v/v) Triton-X 100 in PBS followed by blocking with 5% goat serum in PBS (Merck) for 1 hr at room temperature. Cells were incubated with MF-20 anti-sarcomeric myosin heavy chain IIa IgG mouse antibody supernatant (1:20; Developmental Studies Hydroma Bank, Iowa, USA) in 5% goat serum overnight at 4 ºC. Cells were then incubated with secondary antibody (1:350 Alexa Fluor 488 IgG goat anti-mouse in 5% goat serum) for 1 hr at room temperature. Finally, cells were

incubated with DAPI staining solution for 5 min. Cells were imaged using an inverted fluorescence microscope (Zeiss AXIO, Germany). Image reconstruction was performed using ImageJ software (ImageJ, National Institutes of Health, Bethesda, MD, USA). The fusion index was calculated as the ratio of nuclei number in MF20-positive cells (myotubes) with two or more nuclei divided by the total number of nuclei in each field of view, as previously described [31]. The mean fusion index for each donor was calculated from ten fluorescence microscopy images at 10X magnification.

2.7.4.2 Flow cytometry

Cells cultured in proliferation medium were harvested from the wells, as described in Section 2.4, centrifuged at 190 x *g* and washed with PBS. Cells were stained with Brilliant Violet 711™ anti-human CD56 (NCAM) Antibody (Clone 5.1H11, Biolegend, California, USA), Alexa Fluor® 647 anti-human CD34 Antibody (Clone 561, Biolegend) and PE anti-human CD90 (Thy1) Antibody (Clone 5E10, Biolegend) for 30 min in the dark at RT. Cells were washed once before the analysis. Flow cytometry analysis was performed using BD LSRFortessa™ Cell Analyser (BD Biosciences). Each acquisition file included 20,000 events. The BD FACSDiva™ Software was used for acquisition. Results were analysed using FlowJo™ version 10 software (BD Biosciences).

2.8. Characterization of TIPS PLGA microcarriers after thawing

To evaluate the effect of cryopreservation on the properties of TIPS PLGA microcarriers, the microcarriers (without cells) were incubated and cryopreserved in the same cryoprotectants: i) CS10 or ii) CS10Gr. For the CS10Gr CPA, a 10% GranuGel® (v/v) solution in proliferation medium was freshly prepared. Microcarriers were resuspended in 36 ml proliferation medium, and aliquoted into three 50 ml polypropylene containers as follows: 4 ml for the control samples (before cryopreservation), 16 ml for the CS10 samples, and 16 ml for the CS10Gr samples. For the samples incubated in the CS10, the proliferation medium was removed, and the microcarriers were resuspended in 8 ml CS10. The microcarriers were mixed and quickly aliquoted in eight 2 ml cryogenic vials (1 ml of microcarriers per cryogenic vial). For the samples incubated in the CS10Gr, the proliferation medium was removed, and the microcarriers were resuspended in 4 ml CS10. Using two Luerlock syringes with a connector, the microcarriers were mixed with 4 ml 10% (v/v) GranuGel® solution in proliferation medium. The 8 ml total suspension of microcarriers was quickly aliquoted into eight 2 ml cryogenic vials (1 ml of microcarriers per cryogenic vial). For the process of slow cooling, the ViaFreeze™ controlled rate freezer (Cytiva, Buckinghamshire, UK) with a cooling rate of -1 ºC/min (after 10 min equilibration at 4 ºC) was used. When the temperature reached -70 ºC, the cryogenic vials were transferred to the -70

ºC freezer, and next day they were transferred to the liquid nitrogen, where they were stored for five months.

For the characterization, frozen vials were slowly thawed and left at room temperature for 2 h. The contents of the vials were washed in 10 ml PBS via gentle inversion. Microcarriers were allowed to sediment and washed with 5 ml deionized water. Samples that had not been cryopreserved were used as controls.

2.8.1. Size and morphology of TIPS PLGA microcarriers

The morphological characteristics of the microcarriers after cryopreservation were assessed with a particle analyzer (Morphologi G3).

Scanning electron microscopy (SEM) was used to evaluate the surface morphology of the microcarriers. A drop of the microcarriers was transferred onto an aluminium stub with an adhesive carbon tape and air-dried before sputter coating with gold (Polaron E5000) and imaging using a Hitachi S3400N SEM at 5 keV.

2.8.2 Thermal properties

Differential Scanning Calorimetry (DSC) was used to evaluate the thermal properties of the TIPS PLGA microcarriers after cryopreservation. DSC analysis was conducted using a DSC 25 Differential Scanning Calorimeter (TA Instruments, Delaware, USA). A sample (~1-2 mg) of dried samples was loaded into an aluminum pan and temperature scanning was performed under nitrogen gas according to the following temperature programme: 0ºC → +200 ºC (heating rate: 10 ºC/min) → 0ºC (cooling rate: 10 ºC/min); two cycles). The glass transition (Tg) temperatures were recorded as the midpoint of the thermal transition.

2.9. Statistical analysis

Data were subjected to Kruskal Wallis followed by Dunn's tests for multiple comparisons between pairs of means, using commercially available software (GraphPad Prism). Statistically significant difference between experimental results was indicated by $p < 0.05$ (*), $p < 0.01$ (**), $p < 0.001$ (***), and $p < 0.0001$ (****). Results of cellularized microcarriers are expressed as mean ± standard error of the mean (SEM; n = 5). Results of microcarriers (without cells) are expressed as mean ± standard deviation (SD). Data were analysed using GraphPad Prism version 7 for Windows (GraphPad Software Inc).

3. Results

3.1 Fabrication, cryopreservation and characterization of TIPS PLGA microcarriers

Porous PLGA microcarriers were produced using thermally induced phase separation. The surface of the microcarriers exhibited a heterogeneous hierarchical pore structure characteristic of the TIPS process (Figure 2Ai and 2Av) [32]. The typical differences in the pore structure were observed both within individual microcarriers and between different microcarriers within the same batch. Before culturing with cells, the microcarriers were pre-conditioned to increase their hydrophilic properties. SEM imaging showed that pre-conditioning of the microcarriers resulted in shrinkage without affecting their shape (Figure 2Aii). The surface of the microcarriers retained their porous features typical of TIPS microcarriers (Figure 2Avi).

Incubation of the microcarriers in CS10 cryoprotectant and cryostorage for five months did not change the size and shape of the microcarriers, nor did they collapse or get clustered together. The same was observed for samples incubated in CS10Gr and cryopreserved. Furthermore, the surface morphology and porosity of the samples cryopreserved in CS10 (Figures 2Aiii and 2Avii) or CS10Gr (Figures 2Aiv and 2Aviii) did not change compared with before cryopreservation. All microcarriers retained the porosity and open internal pores.

The mean diameter of the microcarriers produced was ~300 μm (Figure 2Bi). Pre-conditioning of the microcarriers prior to cell attachment resulted in ~36% reduction in size. Microcarriers cryopreserved in CS10 had a diameter reduction of ~ 10% compared to before cryopreservation, while samples cryopreserved in CS10Gr had a diameter reduction of ~ 5%. The reduction in microcarrier diameter was not significantly different between CS10 and CS10Gr samples.

The circularity of microcarriers cryopreserved in CS10 exhibited a higher value compared to the microcarriers before cryopreservation (Figure 2Bii). Microcarriers cryopreserved in CS10Gr had circularity values similar to before cryopreservation. The aspect ratio of the microcarriers was not affected by cryopreservation (Figure 2Biii).

After microcarrier pre-conditioning, DSC revealed a lower Tg (3.0 ºC) compared to the Tg of the microcarriers after fabrication (‘Dry’; Figures 2C and 2D). Post-thawing resulted in a slight increase of Tg (0.3 ºC and 1.3 ºC for microcarriers cryopreserved in CS10 and CS10Gr, respectively) compared to control microcarriers (‘Before cryopreservation’; Tg= 45.6 ºC).

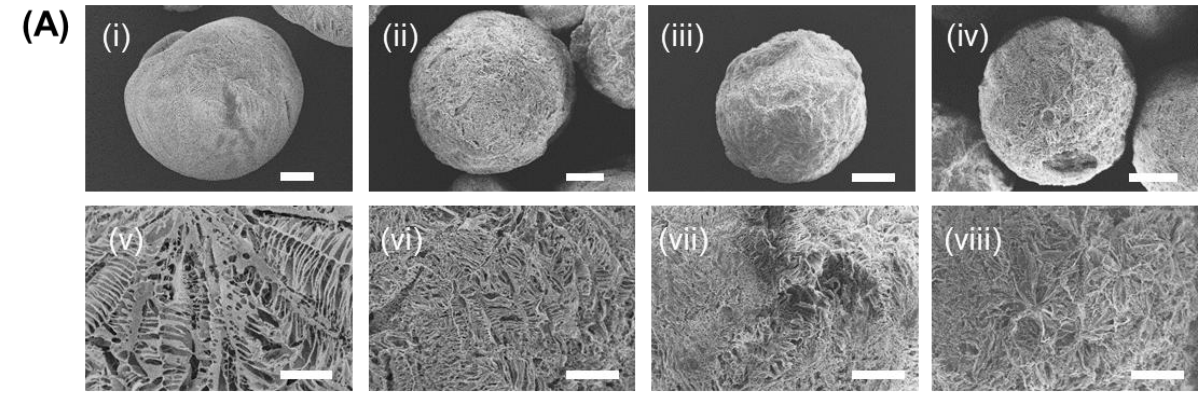

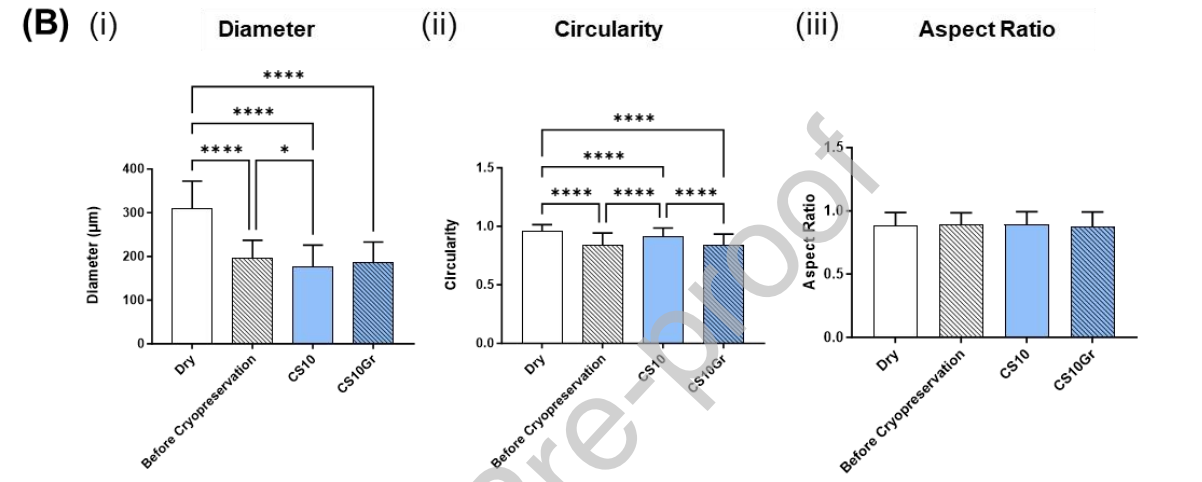

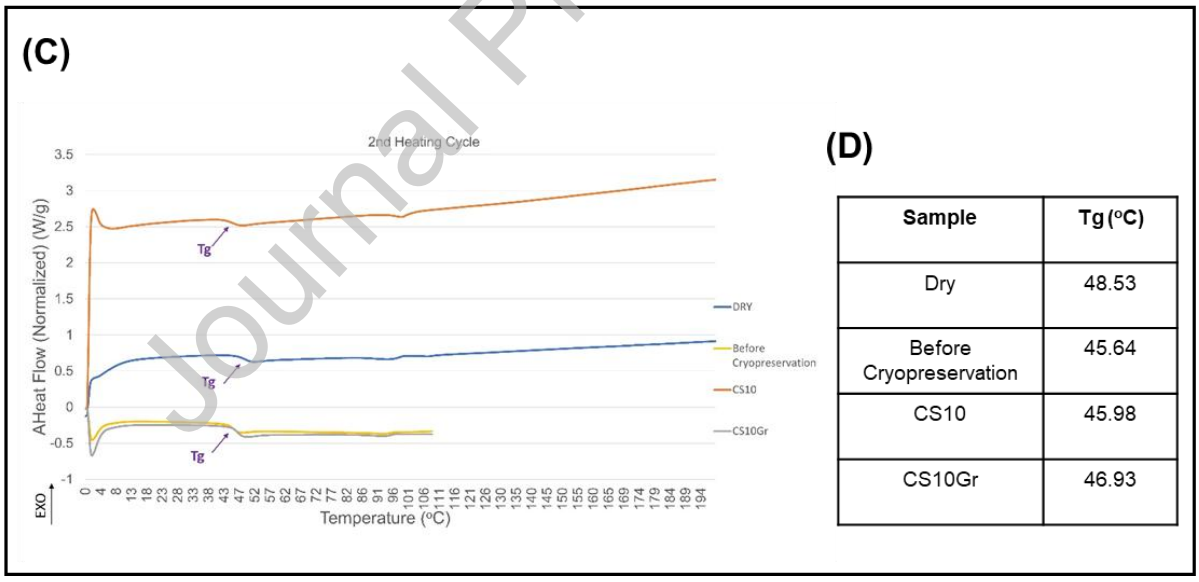

(D)

Sample	Tg (°C)
Dry	48.53
Before Cryopreservation	45.64
CS10	45.98
CS10Gr	46.93

Figure 2: Physical characterization of microcarriers at different stages of cryopreservation and storage. (A) SEM images of dry (untreated control) microcarriers directly after fabrication (Ai and Av), after pre-conditioning ('Before cryopreservation'; Aii and Avi), after incubation in CS10, slow cooling and storage in liquid nitrogen (Aiii and Avii), and after incubation in CS10Gr, slow cooling and storage in liquid nitrogen (Aiv and Aviii) at low (Ai-Aiv) and high (Av-Aviii) magnifications (scale bar in A is 50 µm; in B is 25 µm). (B) Quantitative evaluation of morphological characteristics of the microcarriers at

the different conditions: i) diameter, ii) circularity and iii) aspect ratio (mean ±SD). (C) DSC spectra (2^{nd} heating) of the microcarriers at the different conditions. (D) Thermal glass transition (Tg) points of dry (untreated control) microcarriers, microcarriers before cryopreservation (pre-conditioned), and thawed cryopreserved microcarriers incubated in CS10 or CS10Gr.

3.2. Evaluation of cell viability of the SMDC on TIPS PLGA microcarriers after cryopreservation

After 18 hr incubation in the bioreactor ~95% cells were attached to the microcarriers (Supp. Figure 1). The cellularized microcarriers that had undergone cryopreservation and cryostorage were thawed using two different regimes, i.e. slow (air) or rapid (water), and subsequently assessed at 0 hr and 24 hr post-thawing. Figure 3Ai shows the mean viability (%) value from five different donors. Figure 3Aii shows the results expressed as decrease of viability with respect to the corresponding viability value before cryopreservation. Directly after thawing (0 hr), rapidly thawed cellularized microcarriers had cell viability ≥74% (or ≤21% decrease in cell viability relative to the viability before cryopreservation), whereas cellularized microcarriers thawed slowly had cell viability ≥58% (or ≤38% decrease in cell viability relative to the viability before cryopreservation). There was no statistical significance difference between the samples that had been cryopreserved in CS10 and CS10Gr. At 24 hr post-thawing, cell viability in the rapidly thawed group had cell viability ≥62% (or ≤34% decrease in cell viability relative to the viability before cryopreservation), whereas cellularized microcarriers thawed slowly had cell viability ≥34% (or ≤64% decrease in cell viability relative to the viability before cryopreservation). Overall, samples thawed slowly (9 – 12 min) showed lower viability than cells being thawed rapidly (2 – 3 min).

Cell viability was qualitatively assessed using direct Live/Dead staining. Figure 3B presents the fluorescence microscopy images of samples before cryopreservation (Figures 3Bi and 3Bii) and samples that had been cryopreserved in CS10 (Figures 3Biii and 3Biv) and CS10Gr (Figures 3Bv and 3Bvi) followed by rapid thawing. After cryopreservation there were more dead cells (highlighted with red arrows) compared to before cryopreservation; however, there were still more viable cells than dead cells in both groups.

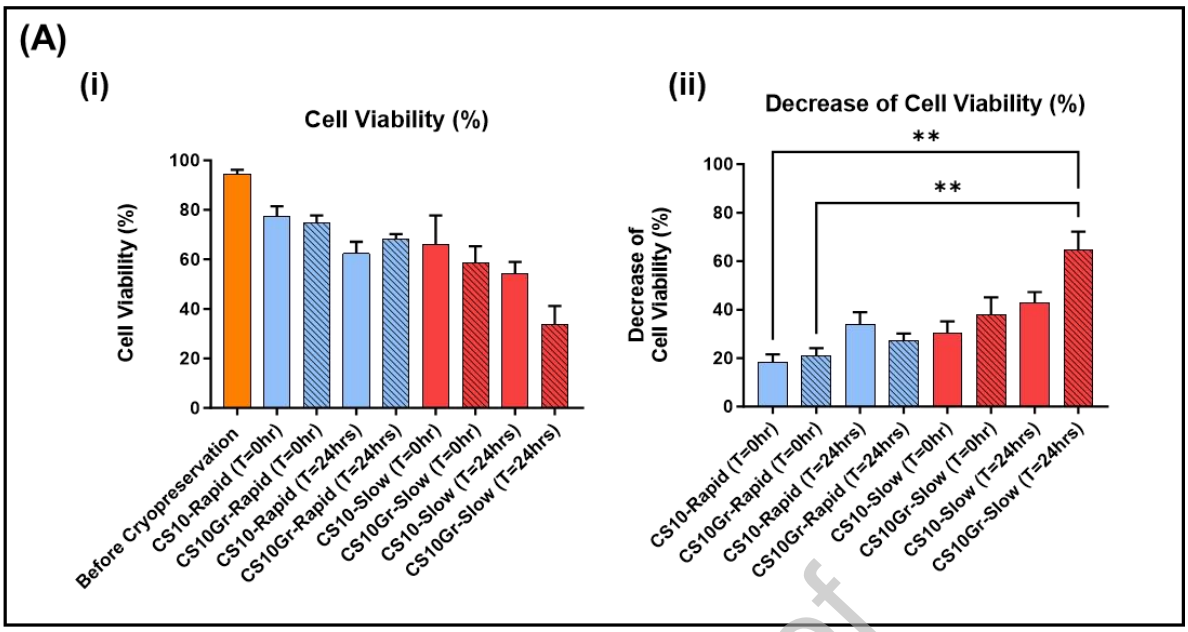

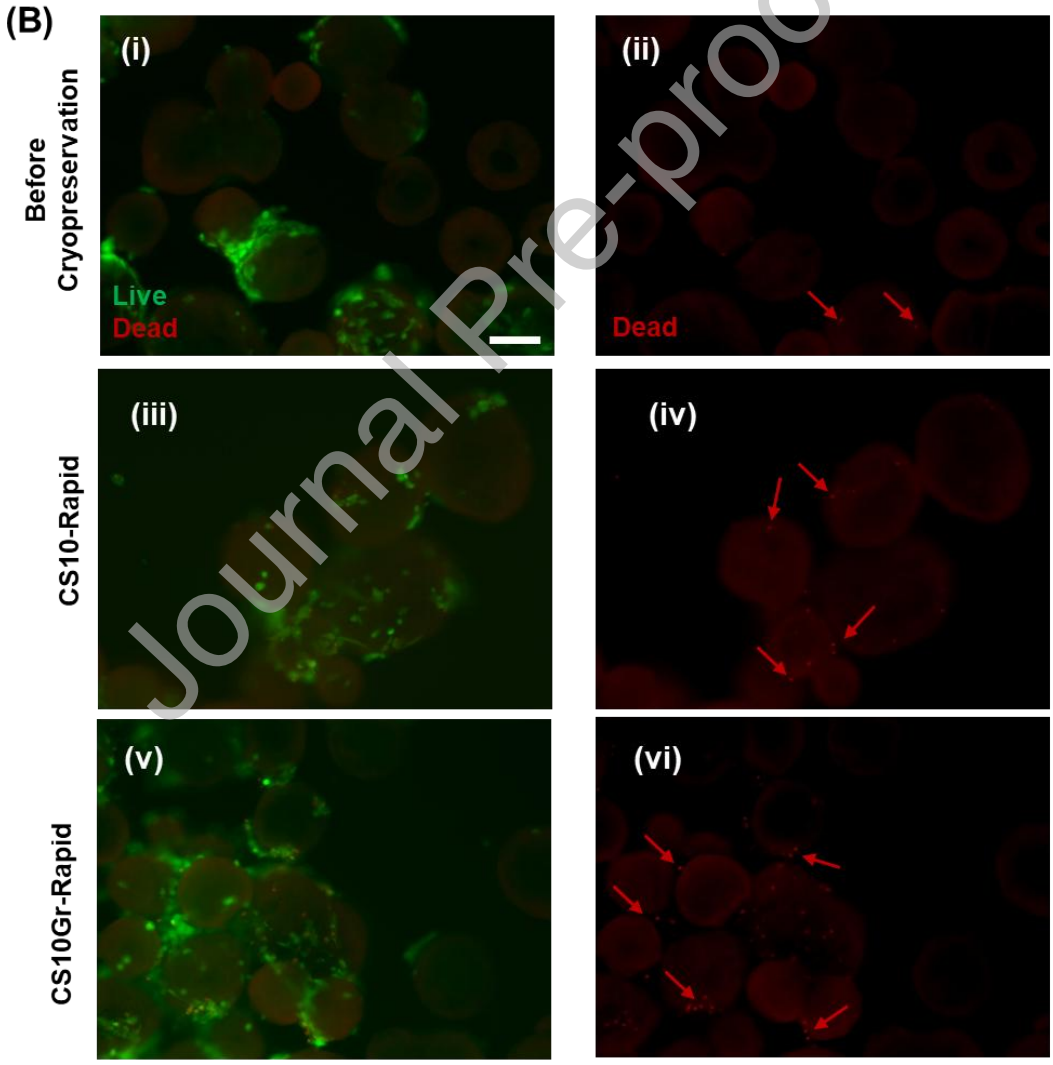

Figure 3: Evaluation of cell viability on the TIPS PLGA microcarriers. (Ai) Viability (%) of attached cells on TIPS PLGA microcarriers for different experimental conditions. (Aii) Decrease of viability (%) of attached cells on TIPS PLGA microcarriers at different experimental conditions with respect to the viability values before cryopreservation. Results are expressed as mean ± standard error for five different donors (SEM; n = 5; **p<0.01). (B) Fluorescence microscopy images of Live/Dead staining of cellularized TIPS PLGA microcarriers before cryopreservation (Bi and Bii) and after thawing of samples cryopreserved in CS10 (Biii and Biv) and CS10 Gr (Bv and Bvi) and rapidly thawed (scale bar is 100 μm).

3.3. Evaluation of cell recovery of SMDC on TIPS PLGA microcarriers after cryopreservation

To assess the total number of cells recovered on the microcarriers after cryopreservation, cells were detached from the microcarriers (Figure 4A). For samples cryopreserved in CS10 and CS10Gr and rapidly thawed, the total cell number was comparable to before cryopreservation. However, the total cell number of cells after cryopreservation in CS10Gr and slow thawing was lower ($p<0.05$) than before cryopreservation.

To assess how cryopreservation affected the number of the cells attached on individual microcarriers, samples from the different experimental conditions were fixed and stained with DAPI directly at 0 hr (Figure 4B) and 24 hr post thawing and the number of cells per microcarrier was subsequently counted. The number of cells per microcarrier was lower in the thawed samples compared to before cryopreservation (Figure 4C).

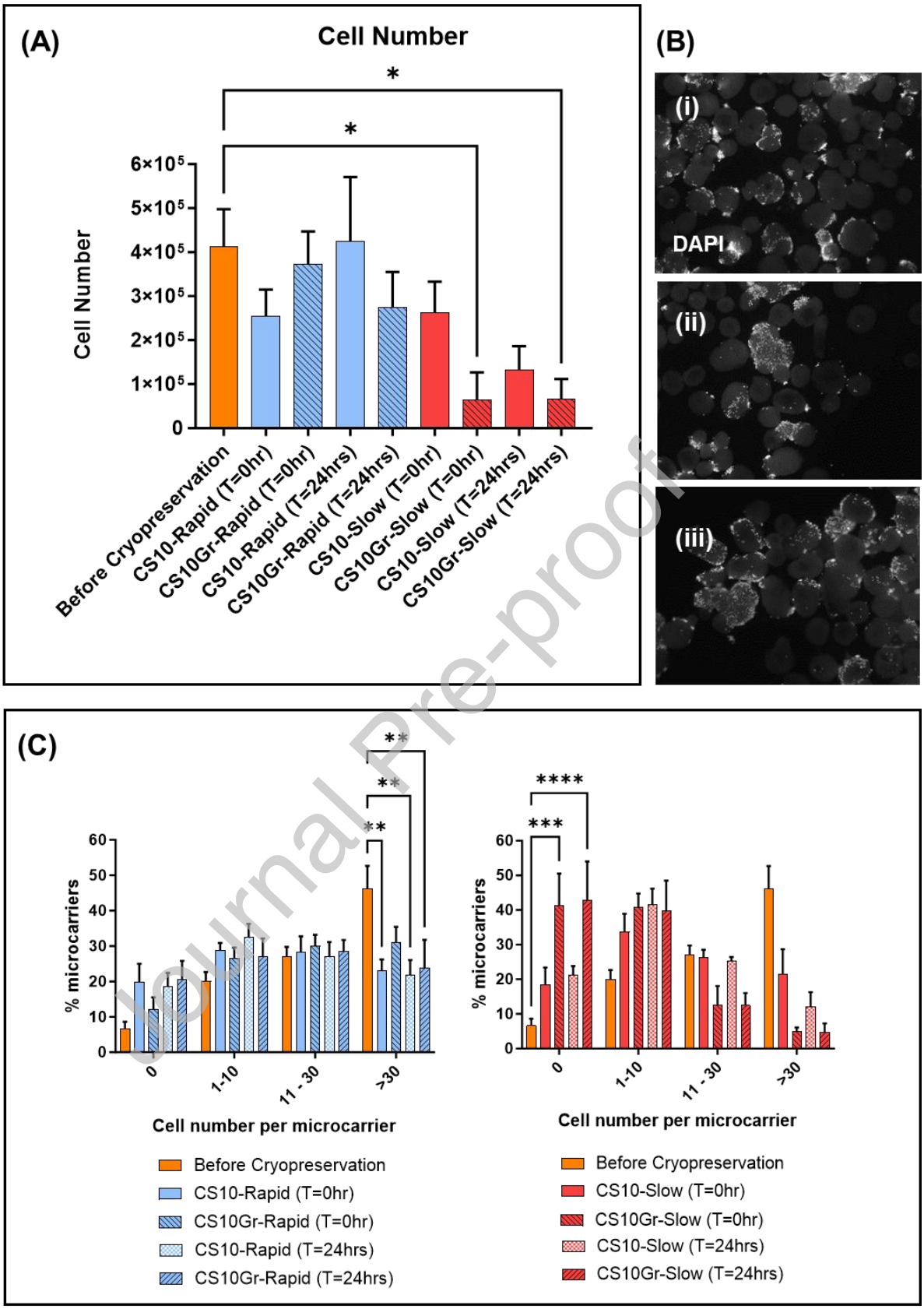

Figure 4: Quantitative evaluation of cell recovery on the TIPS PLGA microcarriers. (A) Number of attached cells on TIPS PLGA microcarriers per cryovial before and after cryopreservation at different

experimental conditions. (B) Fluorescence microscopy images of SMDC cell attached cells on TIPS PLGA microcarriers per cryovial before (Bi) and after cryopreservation in CS10 (Bii) and CS10Gr (Biii) 0 hr post-thawing (grey: DAPI). (C) Number of cells distributed per microcarrier under different experimental conditions. For (A) and (C) results are expressed as mean ± standard error of the mean for five different donors (SEM; n = 5; * p<0.05; **p<0.01; ***p<0.001; ****p<0.0001)

3.4. SMDC differentiation after cryopreservation

After thawing, cells were allowed to migrate off the microcarriers and used for a differentiation assay. Seven days post-onset of differentiation, cells were stained for MHC (Figure 5Ai). Cells in proliferation medium had negative signal for MHC (Figure 5Aii). Regarding the fusion index, cells that had migrated off the microcarriers after cryopreservation for all experimental conditions showed fusion index similar to cells before cryopreservation (Figure 5B). The lowest values were for the cells on the microcarriers that had been cryopreserved in the CS10Gr and slowly thawed.

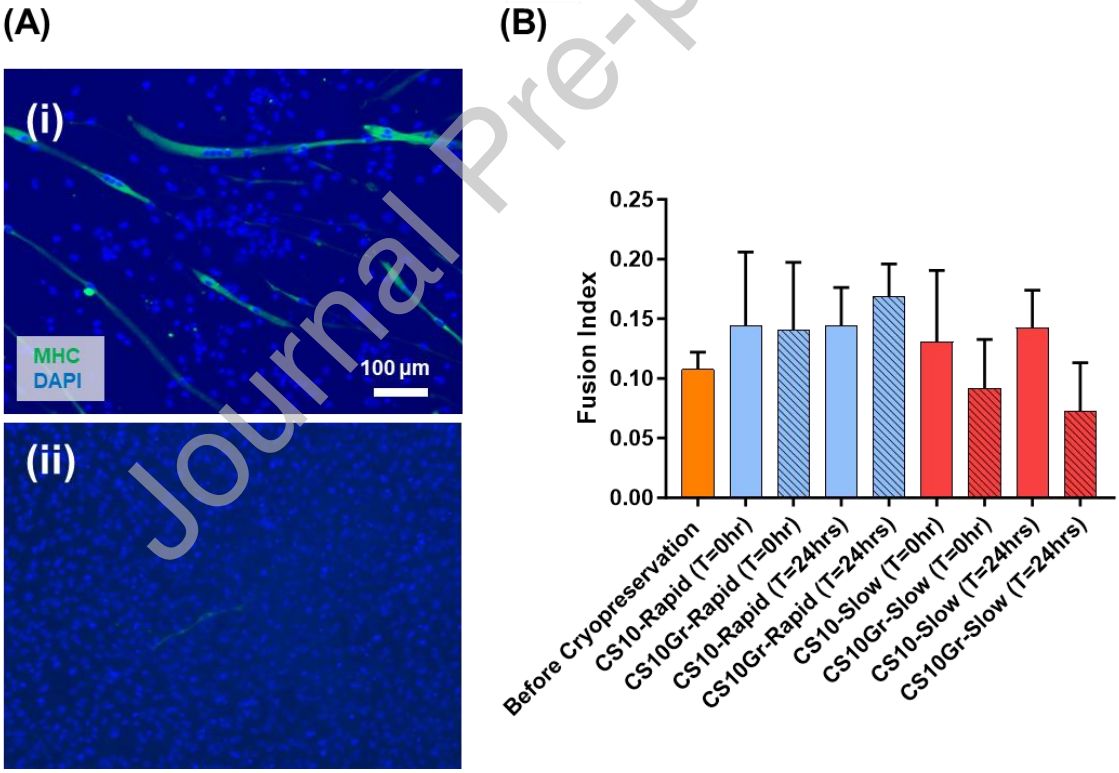

Figure 5: Cell fusion of the SMDC cells after they have migrated off the TIPS PLGA microcarriers and been subjected to different experimental conditions. (A) Fluorescence microscopy images of SMDC cells from one donor after incubation in differentiation medium (i) and proliferation medium (ii). (B)

Cell fusion index following incubation in differentiation medium for 7 days after initial growth and cryopreservation on TIPS PLGA microcarriers under different experimental conditions. Results are expressed as mean ± standard error of the mean for five different donors (SEM; n = 5). There is no statistically significant difference among any groups.

3.5. SMDC surface marker expression after cryopreservation

After thawing, cells were allowed to migrate off the microcarriers and attach to a 6-well plate. Figure 6 shows the expression of the surface markers of the SMDC at the different experimental conditions. There was no difference in the proportion of CD56 positive or CD90 positive cells after cryopreservation compared to before cryopreservation.

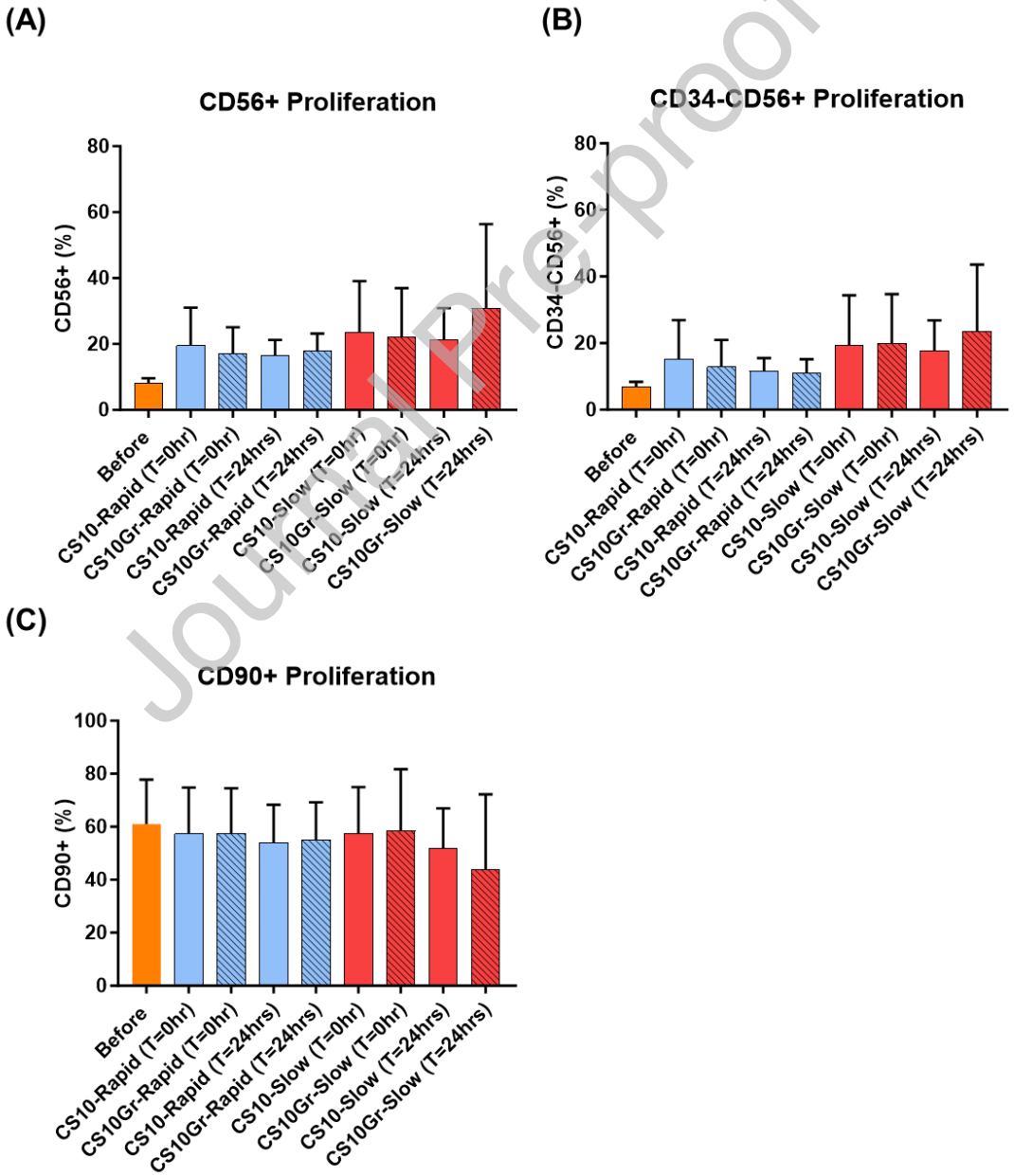

Figure 6: Expression of surface markers on SMDC cells after they have grown on the TIPS PLGA microcarriers under different experimental conditions and incubated in proliferation medium. Results are expressed as mean ± standard error of the mean for five different donors (SEM; n = 5). There was no statistically significant difference among any groups.

4. Discussion

Few studies exist on the effect of cryopreservation of cells attached to microcarriers and there are differing reported outcomes. For example, *Lippens and Cornelissen* tested the effect of different CPA and slow cooling on two different cell types grown for 1 week on CultiSpher-S microcarriers [33]. Average cell viability directly after thawing was 34-42% of the viable cells before cryopreservation for the BMSC and 38-52% for the MC3T3 cells [33]. *Chen et al.* studied the cryopreservation on bone marrow mesenchymal stem cells on novel porous gelatin methacrylamide microcarriers (PMS) and compared them with the commercial Cytodex microcarriers. The study reported a high cell viability (95%) on the PMS microcarriers compared to Cytodex microcarriers (28%) one day post thawing [34]. *Yan et al*. showed a viability of more than 90% hMSC cells after cryopreservation and four days in culture on animal protein-based microcarriers [35]. In all these studies, the method of slow cooling was used. Previous studies have also compared the use of vitrification and slow cooling methods for hMSC [36] and hiPSC [37] attached on alginate microcarriers, reporting higher cell viability with vitrification than slow cooling.

Cryopreservation of adherent cells attached to a substrate surface remains challenging compared with cell suspensions. Adherent cells have both cell-cell and cell-substrate contacts that are sensitive to cryopreservation. Studies with cryopreserved TE constructs highlight additional parameters that may affect post-cryopreservation cell viability and recovery, including construct porosity [38], substrate type [39], storage time [40], cultivation time [41], and combination of different CPA [42]. *Xu et al.* cryopreserved hMSCs attached to different substrates and showed that cells attached to gelatin and Matrigel, but not to glass, survived [39]. Overall, such studies highlight the challenges when using existing cell suspension cryopreservation methods to TE constructs used in combined ATMPs. The current study investigated the effect of two physicochemical parameters that are critical for cell cryopreservation – (i) CPA formulation and (ii) thawing rate.

Two CPA formulations based on the cell-permeating molecule DMSO were investigated. These were: (i) CS10 containing 10% v/v DMSO, and (ii) CS10Gr consisting of CS10 mixed 1:1 with a 10% (v/v) solution of the non-permeating component GranuGel®, an inert hydrogel composed of pectin, sodium carboxymethylcellulose, propylene glycol, and water. The 1:1 mixing of 10% GranuGel® and CS10 diluted both the DMSO and GranuGel® to final concentrations of 5% (v/v). GranuGel® is clinically indicated for the management of partial and full thickness wounds and has been adopted recently as a viscosity modifying carrier vehicle for implantation of the microcarriers in a clinical study investigating their use as a tissue repair scaffold for fistulae. For investigating clinical implantation of cellularized microcarriers as a treatment for incontinence, 5% (v/v) GranuGel® was selected prior to this study as the optimum viscosity for clinical delivery of the product via a syringe and needle. The

same final concentration of GranuGel® (5%) in the cryopreserved product was therefore used in the current study.

The addition of GranuGel® to the cryoprotectant was well tolerated during cryopreservation of the cell-microcarrier combination and may also provide additional benefits by providing a secondary CPA alongside the DMSO. While this is the first study to report the use of GranuGel® with DMSO in a CPA formulation, there is evidence that such secondary non-permeating CPA may stabilise the glassy matrix at ultralow temperatures, preventing cracking in the frozen mixtures during re-warming, which in our case could result in destabilisation of the attached cells and partially degrade the microcarriers [43]. Secondary non-permeating CPA can also allow a reduction in the DMSO concentration whilst retaining good post-thaw recoveries [44].

The proposed delivery concept for cryopreserved microcarriers being investigated in the current study involves thawing and immediate clinical implantation. An intermediate washing stage to remove DMSO from the microcarriers is not included as this could affect the integrity of the product, leading to unintended cell loss that affects the dosage. Each cryovial investigated in the current study contains 1 ml of 10% DMSO (CS10) or 5% DMSO (CS10Gr). This amount of DMSO is far lower than the maximum dose of 1 ml DMSO per kg body weight per day that is considered acceptable for intravenous haematopoietic stem cell transplantation, as advocated by relevant scientific societies, regulatory authorities, and safety data recently reviewed [45]. Nevertheless, further non-clinical safety testing will be required for future clinical testing of the proposed cryopreserved ATMP.

Two warming rates were investigated by thawing frozen vials at 37°C in either a water bath (rapid; 2 – 3 minutes) or in air (slow; 9 – 12 minutes). The thermal conductance of water is higher than air, meaning water transferred heat more easily to the frozen cryovials resulting in faster thawing. Directly after rapid thawing, the viability of cells cryopreserved in CS10 or CS10Gr was higher than the samples that were thawed slowly, indicating the advantage of using a rapid thawing approach for the cell-microcarrier combination. To investigate this further, cell viability was also assessed at 24 hr after thawing to assess potential residual toxic effects of DMSO. At 24 hr post-thawing, a further decrease in cell viability was observed compared with the samples before cryopreservation. For rapid thawing, higher cell viability was observed with samples incubated in CS10Gr compared with samples incubated in CS10. The opposite effect was observed with samples that were slowly thawed, with results indicating that the protective effect of CS10Gr was less effective with slow thawing. These results indicate rapid thawing and the inclusion of a non-permeating agent (GranuGel®) are key to retaining cell viability in the cryopreserved cell-microcarrier combination. The negative effects of slow warming on CS10Gr (final DMSO at 5%) points to a negative effect of the increase in ice fraction as samples warm (compared to CS10 alone). This is likely to be a combination of physical (ice crystal growth) and hypertonic solution when the samples return to the liquid state at around -20°C upwards. Figure 4

clearly shows that number of microcarriers with 0 or only <10 cells at T=0hr after thawing is relatively high in CS10Gr, indicating that the cells have already been displaced at this time-point. Once detached, the anchorage dependent cells in suspension will undergo apoptosis. Based on these findings, further consideration regarding the type of thawing system employed for clinical use of the cryopreserved product is warranted. If the product requires rapid thawing at the point of delivery in a clean environment, the use of a water bath may not be permissible due to the risk of contamination. To avoid this risk, portable dry thawing systems that enable rapid heat transfer and thawing for real-world clinical use are available, such as BioLife Solutions ThawSTAR® CFT2 Automated Thawing System or Barkey plasmatherm™ Cell and Gene.

Another aspect of cell recovery evaluated was the cell number post-thawing compared with before cryopreservation. For the samples that had been warmed rapidly, the number of cells directly after thawing was non-significantly lower for both the CS10 and the CS10Gr samples. 24 hr post thawing, cell number for the samples after rapid thawing was equal to (CS10) or non-significantly lower (CS10Gr) compared with before cryopreservation. The cell number was significantly lower for CS10Gr samples that had been slowly thawed. The results suggest that CS10 protected the cells better than CS10Gr when samples were slowly thawed, whilst this was not evident after rapid rewarming. CS10Gr protected cells when these are thawed quickly but not with slower warming.

To further investigate cell adhesion on the microcarriers, cell count per microcarrier was assessed. The results confirmed use of CS10Gr and slow thawing yielded significantly fewer cells per microcarrier and many microcarriers with no cells attached, suggesting the advantage of rapid rewarming and the higher concentration of DMSO (in the CS10 formulation). The different CPA formulations appeared to have no difference when cells were rapidly thawed. These results emphasize that the time within which thawing is completed is critical. As emphasized by *Fischer et al*., the impact of thawing method is often overlooked [46]. Only a few studies report the effect of thawing rate on cell recovery. By testing different cooling and thawing rates, *Baboo et al.* reported that in slow cooling there is no effect of the thawing rate on the viability of human T cells post thawing [47]. The effect of thawing rate is even less explored in cells attached to a substrate. *Bissoyi and Braslavsky* used focused infrared irradiation enabling thawing times of 1 and 2 sec of cryopreserved Caco2 and RPE cells attached to substrates, showing a superior recovery for 1 sec exposure to irradiation compared with the samples thawed in water bath [48]. However, the 2 s irradiation time had adverse effect.

Cryo-damage induced detachment of cells from substrates has been linked to the elasticity of the substrate [49] or the combined effect of the adhesion time of the cells on the substrate before cryopreservation and the elasticity of the substrate [45]. *Batnyam et al.* studied the cryopreservation of mouse C2C12 myoblasts on an elastic substrate which retains its elasticity at freeze–thawing temperatures. Elastic nanofibrous sheets made of a polymer (i.e. polyurethane), which has a low glass

transition temperature (-30 ºC), were compared to elastic nanofibrous sheets made of a polystyrene (Tg at 106 ºC). It was suggested that cells extending along a nanofiber featuring a low Tg could shrink and still maintain their adhesion to the fiber due to the fiber elasticity, minimizing the detachment that would take place if the deformation was smaller than that of the scaffold [49]. The work of *Meiser et al.* with hiPSCs on alginate microcarriers of two stiffness ranges highlighted the impacts of adhesion time of cells on the microcarriers before cryopreservation and the elasticity of the substrate, which affect the actin cytoskeletal state of the cells [45]. Supra-optimal number of cell adhesion points with a stiff substrate can render the cytoskeleton inelastic and more sensitive to form ice crystals during thawing. If there are not enough adhesion points, cells can lose their connections and detach from the substrate. Such and similar studies could pave the way for novel strategies to improve cryopreservation for TE based constructs.

For ATMPs, it is important to demonstrate that the cellular phenotype of the cryopreserved sample is retained post-thawing. We showed that cryopreserved SMDC migrated off microcarriers *in vitro* and retained their myogenic phenotype using established assays previously used for assessing the phenotype of SMDC used in clinical studies [30,50]. When incubated in myogenic differentiation medium the cells formed multinucleated myotubes positive for MHC. The fusion index after cryopreservation was comparable with the samples before cryopreservation demonstrating cryopreservation did not affect the myogenicity of the cells. Two surface markers used to identify skeletal muscle progenitor cells are CD56 and CD90 (reviewed in [51]). After cryopreservation there was no change to the expression levels for either of these markers compared to cells before cryopreservation, indicating no alteration in the composition of the SMDC cell population. Further investigation of myogenic properties of cells following thawing, such as myotube contractility via calcium transient assays or force transduction experiments, could be used to provide insight into whether cryopreservation affects the force generating functional properties of SMDC.

In addition to the biological phenotype of the attached cells, the integrity of the microcarrier also needs to be assessed [29]. Integrity of the microcarrier following cryopreservation and thawing is important, especially when the microcarriers form an integral component of the tissue engineered product. This includes changes to the shape/size, micro-architecture, and surface porosity. In the present study, incubation of the microcarriers in CPA (CS10 or CS10Gr) and storage at cryogenic temperatures for five months did not change the morphological characteristics of the microcarriers. There was a small decrease in microcarrier diameter, which was more evident in the case of the CS10 compared to CS10Gr, possibly due to the higher DMSO concentration in CS10 compared to the CS10Gr formulation. Importantly, microcarriers retained their shape that enables them to function as a cell carrier for implantation. Also, DMSO present within the two CPA formulations did not cause dissolution of the PLGA microcarriers. Although DMSO has been reported as a solvent for PLGA [52], PLGA dissolution by a solvent, in general, is promoted by lower LA:GA, lower molecular weight (MW) of the polymer

and high temperature of the environment, among other parameters. The PLGA polymer used for the microcarriers had a high (75:25) LA:GA ratio (which implies a stiffer polymer), and also a high MW (95 kg/mol). Furthermore, PLGA microcarriers were in contact with the DMSO at cryogenic temperatures, impacting on its solvent properties.

Changes in the thermal transition point (Tg) of the microcarriers after cryopreservation would reflect a change in polymer rigidity that could impact on the physico-mechanical properties of the microcarriers. The PLGA TIPS microcarriers typically undergo an initial pre-conditioning step to make them hydrophilic and suitable for the cell attachment process. This step was associated with a reduction in the Tg compared with dry control microcarriers, indicating a lowering in the rigidity of the polymer macromolecular chains which would result in softening of the microcarriers before cell attachment. Incubation in CS10 or CS10Gr followed by cryopreservation and thawing caused only a very slight increase in Tg compared with the pre-conditioned microcarriers. Comparing the two different CPA formulations, the higher Tg of the CS10Gr might be attributed to the presence of GranuGel® in the CS10Gr. GranuGel® consists of a blend of polysaccharides that are likely to insert between the macromolecular chains of the PLGA causing a slight increase in rigidity. Overall, Tg results show that the CPA formulations and cryopreservation process investigated did not alter the physico-mechanical properties of the TIPS PLGA microcarriers, which corresponds with the observation that they retained their primary intended function of providing a cell substrate for attachment. Future studies designed to determine the long-term stability of the cryopreserved microcarriers may also include assessment of their mechanical properties such as dynamic mechanical analysis or nanoindentation to evaluate structural stability under physiological conditions when implanted *in vivo*.

In conclusion, the current study demonstrates the technical feasibility of cryopreserving anchorage dependent cells attached to implantable PLGA microcarriers. This approach provides new opportunities to produce tissue engineered constructs composed of cells attached to implantable microcarriers for use as novel combined ATMPs intended for regenerative medicine and resolves significant challenges associated with the distribution of fresh products. In doing so, this approach may increase availability of novel regenerative medicine therapies for a greater number of patients.

References

[1] S. Pina, V.P. Ribeiro, C.F. Marques, F.R. Maia, T.H. Silva, R.L. Reis, J.M. Oliveira, Scaffolding Strategies for Tissue Engineering and Regenerative Medicine Applications, Materials (Basel). 12 (2019) 1824. https://doi.org/10.3390/ma12111824.

[2] P. Bertsch, M. Diba, D.J. Mooney, S.C.G. Leeuwenburgh, Self-Healing Injectable Hydrogels for Tissue Regeneration, Chem. Rev. 123 (2023) 834–873.

https://doi.org/10.1021/acs.chemrev.2c00179.

[3] C.R. Correia, S. Nadine, J.F. Mano, Cell Encapsulation Systems Toward Modular Tissue Regeneration: From Immunoisolation to Multifunctional Devices, Adv. Funct. Mater. 30 (2020) 1908061. https://doi.org/10.1002/adfm.201908061.

[4] S.L. Ding, X. Liu, X.Y. Zhao, K.T. Wang, W. Xiong, Z.L. Gao, C.Y. Sun, M.X. Jia, C. Li, Q. Gu, M.Z. Zhang, Microcarriers in application for cartilage tissue engineering: Recent progress and challenges, Bioact. Mater. 17 (2022) 81–108. https://doi.org/10.1016/j.bioactmat.2022.01.033.

[5] M. Morille, K. Toupet, C.N. Montero-Menei, C. Jorgensen, D. Noël, PLGA-based microcarriers induce mesenchymal stem cell chondrogenesis and stimulate cartilage repair in osteoarthritis, Biomaterials. 88 (2016) 60–69. https://doi.org/10.1016/j.biomaterials.2016.02.022.

[6] C. Duan, M. Yu, C. Hu, H. Xia, R.K. Kankala, Polymeric microcarriers for minimally-invasive cell delivery, Front. Bioeng. Biotechnol. 11 (2023) 1–21. https://doi.org/10.3389/fbioe.2023.1076179.

[7] W. Leong, D.A. Wang, Cell-laden Polymeric Microspheres for Biomedical Applications, Trends Biotechnol. 33 (2015) 653–666. https://doi.org/10.1016/j.tibtech.2015.09.003.

[8] G.S. Major, V.K. Doan, A. Longoni, M.M.M. Bilek, S.G. Wise, J. Rnjak-Kovacina, G.C. Yeo, K.S. Lim, Mapping the microcarrier design pathway to modernise clinical mesenchymal stromal cell expansion, Trends Biotechnol. 42 (2024) 859–876. https://doi.org/10.1016/j.tibtech.2024.01.001.

[9] X.Y. Chen, J.Y. Chen, X.M. Tong, J.G. Mei, Y.F. Chen, X.Z. Mou, Recent advances in the use of microcarriers for cell cultures and their ex vivo and in vivo applications, Biotechnol. Lett. 42 (2020) 1–10. https://doi.org/10.1007/s10529-019-02738-7.

[10] A.-C. Tsai, C.A. Pacak, Bioprocessing of Human Mesenchymal Stem Cells: From Planar Culture to Microcarrier-Based Bioreactors, Bioengineering. 8 (2021) 1–22. https://doi.org/10.3390/bioengineering8070096.

[11] N. Georgi, C. Van Blitterswijk, M. Karperien, Mesenchymal stromal/stem cell-or chondrocyte-seeded microcarriers as building blocks for cartilage tissue engineering, Tissue Eng. - Part A. 20 (2014) 2513–2523. https://doi.org/10.1089/ten.tea.2013.0681.

[12] M. Chen, X. Wang, Z. Ye, Y. Zhang, Y. Zhou, W.S. Tan, A modular approach to the engineering of a centimeter-sized bone tissue construct with human amniotic mesenchymal

stem cells-laden microcarriers, Biomaterials. 32 (2011) 7532–7542. https://doi.org/10.1016/j.biomaterials.2011.06.054.

[13] C. Simitzi, M. Vlahovic, A. Georgiou, Z. Keskin-Erdogan, J. Miller, R.M. Day, Modular Orthopaedic Tissue Engineering With Implantable Microcarriers and Canine Adipose-Derived Mesenchymal Stromal Cells, Front. Bioeng. Biotechnol. 8 (2020) 1–15. https://doi.org/10.3389/fbioe.2020.00816.

[14] E. Dashtimoghadam, F. Fahimipour, N. Tongas, L. Tayebi, Microfluidic fabrication of microcarriers with sequential delivery of VEGF and BMP-2 for bone regeneration, Sci. Rep. 10 (2020) 11764. https://doi.org/10.1038/s41598-020-68221-w.

[15] C. Bouffi, O. Thomas, C. Bony, A. Giteau, M.-C. Venier-Julienne, C. Jorgensen, C. Montero-Menei, D. Noël, The role of pharmacologically active microcarriers releasing TGF-b3 in cartilage formation in vivo by mesenchymal stem cells, Biomaterials. 31 (2010) 6485–6493. https://doi.org/10.1016/j.biomaterials.2010.05.013.

[16] S. Derakhti, S.H. Safiabadi-Tali, G. Amoabediny, M. Sheikhpour, Attachment and detachment strategies in microcarrier-based cell culture technology: A comprehensive review, Mater. Sci. Eng. C. 103 (2019) 109782. https://doi.org/10.1016/j.msec.2019.109782.

[17] P. Dosta, S. Ferber, Y. Zhang, K. Wang, A. Ros, N. Uth, Y. Levinson, E. Abraham, N. Artzi, Scale-up manufacturing of gelatin-based microcarriers for cell therapy, J. Biomed. Mater. Res. - Part B Appl. Biomater. 108 (2020) 2937–2949. https://doi.org/10.1002/jbm.b.34624.

[18] A.M. Fernandes, P.A.N. Marinho, R.C. Sartore, B.S. Paulsen, R.M. Mariante, L.R. Castilho, S.K. Rehen, Successful scale-up of human embryonic stem cell production in a stirred microcarrier culture system, Brazilian J. Med. Biol. Res. 42 (2009) 515–522. https://doi.org/10.1590/S0100-879X2009000600007.

[19] C. Simitzi, E. Hendow, Z. Li, R.M. Day, Promotion of Proangiogenic Secretome from Mesenchymal Stromal Cells via Hierarchically Structured Biodegradable Microcarriers, Adv. Biosyst. 4 (2020) 2000062. https://doi.org/10.1002/adbi.202000062.

[20] A. Bettini, P. Camelliti, D.J. Stuckey, R.M. Day, Injectable biodegradable microcarriers for iPSC expansion and cardiomyocyte differentiation, Adv. Sci. 11 (2024) 1–18. https://doi.org/10.1002/advs.202404355.

[21] A.L. Cartaxo, A. Fernandes-Platzgummer, C.A.V. Rodrigues, A.M. Melo, K. Tecklenburg, E. Margreiter, R.M. Day, C.L. da Silva, J.M.S. Cabral, Developing a Cell-Microcarrier Tissue-Engineered Product for Muscle Repair Using a Bioreactor System, Tissue Eng. - Part C Methods. 29 (2023) 583–595. https://doi.org/10.1089/ten.tec.2023.0122.

[22] B. Bai, C. Xue, Y. Wen, J. Lim, Z. Le, Y. Shou, S. Shin, A. Tay, Cryopreservation in the Era of Cell Therapy: Revisiting Fundamental Concepts to Enable Future Technologies, Adv. Funct. Mater. 33 (2023) 2303373. https://doi.org/10.1002/adfm.202303373.

[23] J. Meneghel, P. Kilbride, G.J. Morris, Cryopreservation as a Key Element in the Successful Delivery of Cell-Based Therapies—A Review, Front. Med. 7 (2020) 1–17. https://doi.org/10.3389/fmed.2020.592242.

[24] T.H. Jang, S.C. Park, J.H. Yang, J.Y. Kim, J.H. Seok, U.S. Park, C.W. Choi, S.R. Lee, J. Han, Cryopreservation and its clinical applications, Integr. Med. Res. 6 (2017) 12–18. https://doi.org/10.1016/j.imr.2016.12.001.

[25] M.M. Taherian, P. Abdoos, M.H. Taherian, F. Ghorbanian, Z. Saltanatpour, A. Alizadeh, Cryopreservation of Stem Cells in Tissue Engineering and Regenerative Medicine, J. Appl. Biotechnol. Reports. 11 (2024) 1359–1370. https://doi.org/10.30491/jabr.2022.331200.1501.

[26] R. Li, R. Johnson, G. Yu, D.H. McKenna, A. Hubel, Preservation of cell-based immunotherapies for clinical trials, Cytotherapy. 21 (2019) 943–957. https://doi.org/10.1016/j.jcyt.2019.07.004.

[27] K.A. Murray, M.I. Gibson, Chemical approaches to cryopreservation, Nat. Rev. Chem. 6 (2022) 579–593. https://doi.org/10.1038/s41570-022-00407-4.

[28] B. Fuller, R. Fleck, G. Stacey, Innovation in cryopreservation & cold chain management, Cell Gene Ther. Insights. 10 (2024) 1407–1422. https://doi.org/10.18609/cgti.2024.184.

[29] I. Arutyunyan, A. Elchaninov, G. Sukhikh, T. Fatkhudinov, Cryopreservation of Tissue-Engineered Scaffold-Based Constructs: from Concept to Reality, Stem Cell Rev. Reports. 18 (2022) 1234–1252. https://doi.org/10.1007/s12015-021-10299-4.

[30] A. Frudinger, R. Marksteiner, J. Pfeifer, E. Margreiter, J. Paede, M. Thurner, Skeletal muscle-derived cell implantation for the treatment of sphincter-related faecal incontinence, Stem Cell Res. Ther. 9 (2018) 1–20. https://doi.org/10.1186/s13287-018-0978-y.

[31] C. Desprez, D. Danovi, C.H. Knowles, R.M. Day, Cell shape characteristics of human skeletal muscle cells as a predictor of myogenic competency: A new paradigm towards precision cell therapy, J. Tissue Eng. 14 (2023) 1–18. https://doi.org/10.1177/20417314221139794.

[32] J.J. Blaker, J.C. Knowles, R.M. Day, Novel fabrication techniques to produce microspheres by thermally induced phase separation for tissue engineering and drug delivery, Acta Biomater. 4 (2008) 264–272. https://doi.org/10.1016/j.actbio.2007.09.011.

[33] E. Lippens, M. Cornelissen, Slow cooling cryopreservation of cell-microcarrier constructs,

Cells Tissues Organs. 192 (2010) 177–186. https://doi.org/10.1159/000313419.

[34] X. Chen, D. Zhang, X. Wang, Z. Liu, H. Kang, C. Liu, F. Chen, Preparation of porous GelMA microcarriers by microfluidic technology for Stem-Cell culture, Chem. Eng. J. 477 (2023) 146444. https://doi.org/10.1016/j.cej.2023.146444.

[35] X. Yan, K. Zhang, Y. Yang, D. Deng, C. Lyu, H. Xu, W. Liu, Y. Du, Dispersible and Dissolvable Porous Microcarrier Tablets Enable Efficient Large-Scale Human Mesenchymal Stem Cell Expansion, Tissue Eng. - Part C Methods. 26 (2020) 263–275. https://doi.org/10.1089/ten.tec.2020.0039.

[36] Y. Wu, F. Wen, S.S. Gouk, E.H. Lee, L.L. Kuleshova, Cryopreservation strategy for tissue engineering constructs consisting of human mesenhymal stem cells and hydrogel biomaterials, Cryo Letters. 36 (2015) 325–335.

[37] I. Meiser, J. Majer, A. Katsen-Globa, A. Schulz, K. Schmidt, F. Stracke, E. Koutsouraki, G. Witt, O. Keminer, O. Pless, J. Gardner, C. Claussen, P. Gribbon, J.C. Neubauer, H. Zimmermann, Droplet-based vitrification of adherent human induced pluripotent stem cells on alginate microcarrier influenced by adhesion time and matrix elasticity, Cryobiology. 103 (2021) 57–69. https://doi.org/10.1016/j.cryobiol.2021.09.010.

[38] P.F. Costa, A.F. Dias, R.L. Reis, M.E. Gomes, Cryopreservation of cell/scaffold tissue-engineered constructs, Tissue Eng. - Part C Methods. 18 (2012) 852–858. https://doi.org/10.1089/ten.tec.2011.0649.

[39] X. Xu, Y. Liu, Z.F. Cui, Effects of cryopreservation on human mesenchymal stem cells attached to different substrates, J Tissue Eng Regen Med. 8 (2014) 664–672. https://doi.org/10.1002/term.1570.

[40] M.N. Egorikhina, Y.P. Rubtsova, D.Y. Aleynik, Long-term cryostorage of mesenchymal stem cell-containing hybrid hydrogel scaffolds based on fibrin and collagen, Gels. 6 (2020) 1–12. https://doi.org/10.3390/gels6040044.

[41] A. Katsen-Globa, I. Meiser, Y.A. Petrenko, R. V. Ivanov, V.I. Lozinsky, H. Zimmermann, A.Y. Petrenko, Towards ready-to-use 3-D scaffolds for regenerative medicine: Adhesion-based cryopreservation of human mesenchymal stem cells attached and spread within alginate-gelatin cryogel scaffolds, J. Mater. Sci. Mater. Med. 25 (2014) 857–871. https://doi.org/10.1007/s10856-013-5108-x.

[42] H. Gurruchaga, L. Saenz Del Burgo, A. Garate, D. Delgado, P. Sanchez, G. Orive, J. Ciriza, M. Sanchez, J.L. Pedraz, Cryopreservation of Human Mesenchymal Stem Cells in an Allogeneic Bioscaffold based on Platelet Rich Plasma and Synovial Fluid, Sci. Rep. 7 (2017)

1–12. https://doi.org/10.1038/s41598-017-16134-6.

[43] G.D. Elliott, S. Wang, B.J. Fuller, Cryoprotectants: A review of the actions and applications of cryoprotective solutes that modulate cell recovery from ultra-low temperatures, Cryobiology. 76 (2017) 74–91. https://doi.org/10.1016/j.cryobiol.2017.04.004.

[44] P.S. Steif, D.A. Noday, Y. Rabin, Can Thermal Expansion Differences between Cryopreserved Tissue and Cryoprotective Agents Alone Cause Cracking ?, Cryo Letters. 30 (2009) 414–421.

[45] E. Niebergall-Roth, M.A. Kluth, Dimethyl sulfoxide in cryopreserved mesenchymal stromal cell therapy products: is there a safety risk to patients?, J. Transl. Med. 23 (2025) 932-952. https://doi.org/10.1186/s12967-025-06807-6

[46] B. Fischer, Walking on thin ice: controlled freezing & thawing of pharmaceutical active molecules, Cell Gene Ther. Insights. 8 (2022) 1457–1464. https://doi.org/10.18609/cgti.2022.212.

[47] J. Baboo, P. Kilbride, M. Delahaye, S. Milne, F. Fonseca, M. Blanco, J. Meneghel, A. Nancekievill, N. Gaddum, G.J. Morris, The Impact of Varying Cooling and Thawing Rates on the Quality of Cryopreserved Human Peripheral Blood T Cells, Sci. Rep. 9 (2019) 1–13. https://doi.org/10.1038/s41598-019-39957-x.

[48] A. Bissoyi, I. Braslavsky, Adherent cell thawing by infrared radiation, Cryobiology. 103 (2021) 129–140. https://doi.org/10.1016/j.cryobiol.2021.08.002.

[49] O. Batnyam, S.I. Suye, S. Fujita, Direct cryopreservation of adherent cells on an elastic nanofiber sheet featuring a low glass-transition temperature, RSC Adv. 7 (2017) 51264–51271. https://doi.org/10.1039/c7ra10604a.

[50] M. Thurner, F. Asim, D. Garczarczyk-Asim, K. Janke, M. Deutsch, E. Margreiter, J. Troppmair, R. Marksteiner, Development of an in vitro potency assay for human skeletal muscle derived cells. PLOS ONE 13(2018): e0194561. https://doi.org/10.1371/journal.pone.0194561

[51] S.-R. Tey, S. Robertson, E. Lynch, M. Suzuki, Coding Cell Identity of Human Skeletal Muscle Progenitor Cells Using Cell Surface Markers: Current Status and Remaining Challenges for Characterization and Isolation, Front. Cell Dev. Biol. 7 (2019) 1–27. https://doi.org/10.3389/fcell.2019.00284.

[52] L.H. Hung, S.Y. Teh, J. Jester, A.P. Lee, PLGA micro/nanosphere synthesis by droplet microfluidic solvent evaporation and extraction approaches, Lab Chip. 10 (2010) 1820–1825. https://doi.org/10.1039/c002866e.

Acknowledgements:

The authors gratefully acknowledge the financial support through the European Union's Horizon 2020 research and innovation programme under grant agreement No 874807 and through the Medical Research Council under the 'Gap Fund for early-stage development of new healthcare interventions' award (Ref: UKRI801). We would like to thank Mr. Jamie Evans for their technical support with flow cytometry and Dr. George Georgiou for their technical support with differential scanning calorimetry. BioRender was used to produce schematic elements in Figure 1.

Authors' contributions

CS designed and conducted the experiments involving SMDC and/or TIPS PLGA microcarriers, analyzed the data, interpreted results and drafted the manuscript. JZ fabricated the TIPS PLGA microcarriers and performed some of the experiments of MorphologiG3. RM provided the SMDC and edited the manuscript. BF designed the experiments, interpreted results and edited the manuscript. RD conceived the study, designed the experiments, fabricated the TIPS PLGA microcarriers, interpreted results, and edited the manuscript. All authors reviewed the manuscript.

Declaration of interest statement

RD is a Director and employee of a company that produces 3D biomaterials for therapeutic applications. BF acts as a cryobiology advisor (pro bono) to industry. RM is a Director and employee of Innovacell. None of the other authors have declarations of interest.